

## Optical reflectivity and Raman spectra of $\text{Sr}_2\text{FeO}_4$ under pressure

P. Adler, A.F. Goncharov,\* K. Syassen, and E. Schönherr

*Max-Planck-Institut für Festkörperforschung, Heisenbergstrasse 1, D-70569 Stuttgart, Germany*

(Received 22 March 1994; revised manuscript received 6 July 1994)

We have investigated the effect of pressure on the optical reflectivity (0.5 – 4 eV,  $T=300$  K) and Raman spectra ( $T=20 - 300$  K) of  $\text{Sr}_2\text{FeO}_4$ , an insulating compound with iron in the high oxidation state +4. The lowest optical transition near 1.2 eV shifts to lower energy with increasing pressure, and the overall near-infrared oscillator strength starts to increase significantly for pressures above 6 GPa. This behavior is interpreted in terms of a gap narrowing between a local  ${}^5E_g$  ground state and a  $d^5L^{-1}$ -like continuum possibly followed by an insulator-metal transition. In addition to the phonon Raman modes, which are allowed in the  $\text{K}_2\text{NiF}_4$ -type crystal structure, we observe a broad Raman band near  $350\text{ cm}^{-1}$ . This band develops into a sharp feature upon cooling to 20 K and vanishes in a narrow pressure range around 5.5 GPa. Oxygen isotope substitution experiments prove that the band is related to oxygen vibrations. We consider explanations where the  $350\text{ cm}^{-1}$  mode arises from spin-induced phonon scattering or from small structural displacements of Fe ions.

### I. INTRODUCTION

The physics and chemistry of the first transition-metal (TM) series is determined by the large on-site  $d$ - $d$  Coulomb interaction. This Coulomb interaction leads to the possibility of insulating ground states in the case of partially filled  $d$  shells where metallic behavior is expected in the framework of one-electron band structure theories. Classical examples are the simple TM oxides FeO, CoO, and NiO.<sup>1,2</sup> Systematic investigations of the electronic structure of TM halides and chalcogenides<sup>3-6</sup> using optical and high-energy spectroscopies have resulted in an increased understanding of how the ground state depends on the nature of the TM ion, its oxidation state, the chemical nature of the anion, and the crystal structure.

Experimental results are frequently analyzed within a cluster configuration interaction (CI) approach which takes into account explicitly the metal- $3d$ -ligand- $p$  hybridization. The CI approach extends the ligand-field formalism by constructing the wave functions for an  $[\text{MX}_n]^{z-}$  cluster as a linear combination of  $d^n$ ,  $d^{n+1}L^{-1}$ ,  $d^{n+2}L^{-2}$ , etc. configurations where  $d^n$  corresponds to the ionic limit and the notation  $L^{-m}$  denotes  $m$  holes in the ligand  $p$  orbitals. From the analysis of high-energy spectra the charge-transfer energy  $\Delta$  for  $3d^n \rightarrow 3d^{n+1}L^{-1}$  fluctuations, the correlation energy  $U$  for  $3d^n + 3d^n \rightarrow 3d^{n-1} + 3d^{n+1}$  fluctuations, and the  $p$ - $d$  hybridization matrix element  $T_{pd}$  are derived. The actual electronic behavior of the crystal depends on the relative strengths of intracenter and intercenter interactions.<sup>7</sup> The latter are determined by the crystal structure and lead to dispersal widths  $W_d$  and  $W_p$  for the TM  $d$  and ligand  $p$  states.

The different situations occurring in TM compounds have been summarized in the Zaanen-Sawatzky-Allen scheme.<sup>8</sup> Depending on the relative magnitude of the parameters, TM compounds may be Mott insulators

( $W_d < U < \Delta$ ),  $d$ -band metals ( $U < \Delta$  and  $W_d > U$ ), charge-transfer insulators [ $\Delta < U$  and  $(W_p + W_d)/2 < \Delta$ ], or ligand- $p$ -band metals [ $\Delta < U$  and  $(W_p + W_d)/2 > \Delta$ ].

In general  $\Delta$  decreases from the left to the right hand side of the TM series and with increasing oxidation state for a given TM ion.<sup>4</sup> In the case of TM ions with high formal oxidation states, these trends may lead to negative  $\Delta$  values and dominant  $d^{n+1}L^{-1}$  contributions rather than ionic  $d^n$  contributions in the wave function of the ground state. An example which has found interest recently in connection with the  $p$ -doped cuprate superconductors is the insulator  $\text{NaCuO}_2$  with copper in the +3 oxidation state.<sup>7</sup>

Remarkable electronic properties are found for oxoferrates with iron in the +4 oxidation state.<sup>9</sup> The stoichiometric perovskite  $\text{SrFeO}_3$  (Refs. 10 and 11) is metallic down to 4 K and orders antiferromagnetically below 130 K. From a cluster model analysis of Fe  $2p$  photoelectron spectra the electronic structure parameters  $\Delta_{\text{eff}} = -3.1$  eV,  $U_{\text{eff}} = 7$  eV, and  $T_\sigma = 2.2$  eV were derived,<sup>12</sup> leading to a  ${}^5E_g$  ground state with dominant  $d^5L^{-1}$  character for an  $[\text{FeO}_6]^{8-}$  cluster. The parameters  $\Delta_{\text{eff}}$  and  $U_{\text{eff}}$  refer to the lowest-energy multiplet components and include the exchange stabilization of the  $d^5$  configuration. Mössbauer spectra of  $\text{SrFeO}_3$  reveal a single  $\text{Fe}^{4+}$  site above as well as below  $T_N$ . The slightly distorted perovskite  $\text{CaFeO}_3$ ,<sup>13,14</sup> on the other hand, is an antiferromagnetic semiconductor ( $T_N \approx 120$  K). The Mössbauer spectra of  $\text{CaFeO}_3$  evidence two different sites with considerably different isomer shifts and hyperfine fields. This has been interpreted in terms of a  $2\text{Fe}^{4+} \rightarrow \text{Fe}^{3+} + \text{Fe}^{5+}$  valence disproportionation.

Recently the properties of the  $\text{K}_2\text{NiF}_4$ -type oxide  $\text{Sr}_2\text{FeO}_4$ , a compound isotopic with the superconductors  $\text{La}_{2-x}\text{Sr}_x\text{CuO}_4$ , have been investigated.<sup>15,16</sup> The tetragonal crystal structure (space group  $I4/mmm$ ) contains the tetravalent iron atoms in the center positions

of slightly elongated oxygen octahedra (site symmetry  $D_{4h}$ ) with the apical iron-oxygen bond distances being about 2 pm larger than the equatorial ones.<sup>17</sup> In agreement with the general trends found when quasi-two-dimensional  $K_2NiF_4$ -type systems are compared with the three-dimensional perovskites,<sup>18</sup>  $Sr_2FeO_4$  is an antiferromagnetic semiconductor with a higher resistivity and a lower magnetic ordering temperature ( $T_N \approx 60$  K) compared to  $SrFeO_3$ . The Mössbauer spectra reveal a single  $Fe^{4+}$  site above  $T_N$  but at least four inequivalent  $Fe^{4+}$  sites below  $T_N$ .<sup>15,16</sup> The isomer shifts of the different sites, however, are identical, so that a valence disproportionation can be excluded.

The higher electronic conductivity of  $SrFeO_3$  compared to  $Sr_2FeO_4$  is presumably a consequence of a larger bandwidth  $W$  arising from the three-dimensional intercluster interactions. Application of external pressure should result in an increase of  $W$  for  $Sr_2FeO_4$ . This is expected to lead to a gap narrowing or even an insulator-metal transition. Alternatively, a pressure-induced high-spin-low-spin transition may occur as was recently found for  $CaFeO_3$  at 30 GPa by pressure-dependent Mössbauer spectroscopy.<sup>19</sup>

In this work we report a high-pressure investigation of  $Sr_2FeO_4$  using optical reflectivity measurements at room temperature and temperature- and pressure-dependent Raman spectroscopy. Reflectivity data evidence pressure-induced changes of the electronic structure which are consistent with a band gap narrowing and an insulator - metal transition occurring near 6 GPa. Below this pressure the Raman spectra show a low-energy excitation near  $350\text{ cm}^{-1}$ , which is not related to any Raman-allowed phonon mode of the  $K_2NiF_4$ -type crystal structure. Furthermore, this mode exhibits a pronounced narrowing upon cooling and an isotope shift if  $^{16}O$  is replaced by  $^{18}O$ . Different possibilities for the origin of this mode are considered.

## II. EXPERIMENTAL DETAILS

$Sr_2FeO_4$  was prepared from  $SrO$  and  $Fe_2O_3$  at  $650^\circ\text{C}$  in flowing oxygen atmosphere. Details are given elsewhere.<sup>15</sup> The sample was characterized by x-ray powder diffractometry and room temperature Mössbauer spectroscopy. The x-ray diagram revealed the presence of a small amount of unreacted  $\alpha\text{-Fe}_2\text{O}_3$  besides the  $K_2NiF_4$ -type phase  $Sr_2FeO_4$  [lattice constants:  $a = 386.4(1)$  pm,  $c = 1240.4(2)$  pm]. This is in accord with the Mössbauer spectrum which shows a weak  $Fe^{3+}$  magnetic hyperfine sextet [isomer shift  $\delta$  relative to  $\alpha\text{-iron} = 0.39(2)$  mm  $s^{-1}$ , hyperfine field  $B_{hf} = 52.45(10)$  T] in addition to the  $Fe^{4+}$  quadrupole doublet [ $\delta = -0.014(1)$  mm  $s^{-1}$ , quadrupole splitting  $\Delta E_Q = 0.442(2)$  mm  $s^{-1}$ ]. Within error limits these parameters are identical to those for a  $Sr_2FeO_4$  sample which was later annealed under an oxygen pressure of 40 MPa. Therefore it is concluded that the sample prepared at 0.1 MPa oxygen atmosphere, which was used for the present study, did not contain major  $Fe^{3+}$  contributions within the  $K_2NiF_4$ -type phase.  $Fe^{3+}$  contents of up to 3% would be within the detection limit of the Mössbauer spectrum. For as-

sisting the assignment of the Raman spectra an isotope exchange of  $^{18}O$  for  $^{16}O$  was performed by heating a sample of  $Sr_2Fe^{16}O_4$  in an  $^{18}O_2$  gas atmosphere for 4 days. From gravimetric data an isotope exchange of at least 80% was estimated. The x-ray powder diagram, lattice constants, and the Mössbauer spectrum of the  $^{18}O$  sample agreed within error limits with those of the  $^{16}O$  sample.

High-pressure optical reflectivity spectra were measured at 300 K using a diamond anvil cell (DAC) in combination with a micro-optical system similar to that employed in previous high-pressure reflectivity studies.<sup>20–22</sup> The sample was first prepressed in order to produce a smooth surface and then mounted in the pressure cell such that the smooth surface was in direct contact with one of the diamond windows. The remaining sample volume was filled with CsCl serving as a quasihydrostatic pressure medium. In this experiment we measure the absolute reflectivity at near-normal incidence (denoted  $R_d$ ) at the diamond-sample interface from a focal spot of about  $30\ \mu\text{m}$  diameter. The normalized  $R_d$  spectra reported below are corrected for absorption in the diamond window and for reflection losses at its external surface. Raman spectra were measured at temperatures between 20 and 300 K with the DAC placed in a continuous flow helium cryostat. In these studies condensed helium served as a pressure-transmitting medium in order to provide fully hydrostatic conditions even at low temperatures. Raman spectra were excited by Ar and Kr ion laser lines ( $\lambda_{ex} = 514.5$  nm, 530.9 nm, and 568.2 nm). Spectra were measured in near-backscattering geometry employing a triple spectrograph and a multichannel detector. The laser radiation was focused down to a spot of about  $80\ \mu\text{m}$  diameter. The laser power on the sample was always kept below 5 mW in order to avoid laser heating. Pressure was measured by the ruby luminescence method<sup>23</sup> using the temperature correction given in Ref. 24.

## III. EXPERIMENTAL RESULTS

Figure 1 shows optical reflectivity spectra of  $Sr_2FeO_4$  measured at different pressures. In the low-pressure range ( $P = 4$  GPa) we observe a well-defined reflectivity maximum near 1.15 eV and a broader band centered at about 3 eV. With increasing pressure the low-energy peak shows a redshift of roughly  $-0.05(1)$  eV/GPa. In addition, at about 6 GPa the near-infrared reflectivity starts to increase continuously. This increase saturates at about 20 GPa and further raising the pressure to 38 GPa results in only minor changes in the reflectivity spectra. The reflectivity minimum near 1.8 eV remains pinned at this energy, and the 3 eV band does not shift significantly, but broadens somewhat under pressure. The pinning of the reflectivity edge near 1.8 eV is obviously due to screening effect from higher-energy excitations. The pressure-induced changes in the optical reflectivity are reversible upon releasing pressure.

We have simulated the reflectivity spectra by using a superposition of Drude-Lorentz oscillators for the complex dielectric function, which is then substituted into the

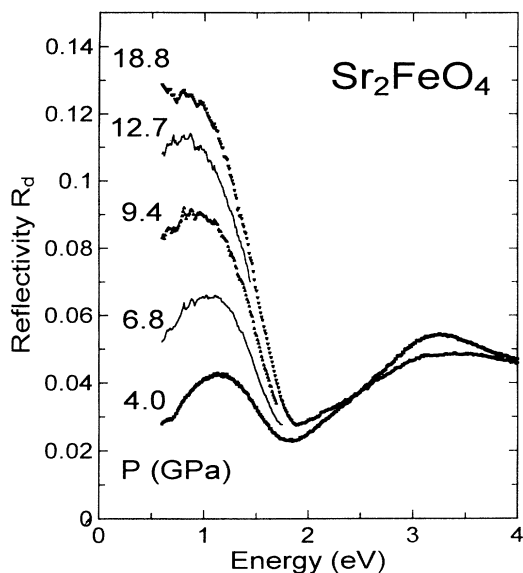


FIG. 1. Reflectivity spectra of  $\text{Sr}_2\text{FeO}_4$  at different pressures. The absolute reflectivity  $R_d$  refers to that measured at the sample-diamond interface (see text for details).

Fresnel equation for the normal incidence reflectivity. We allowed for a total oscillator strength below 10 eV which is similar to that derived from the optical response of semiconducting cuprates.<sup>22</sup> In other words, the effective number of electrons contributing to the imaginary part of the dielectric function below 10 eV has been fixed, such that the integrated optical conductivity between 0 and 10 eV corresponds to an effective electron number<sup>25</sup> of  $0.07/\text{\AA}^3$ . In this way we have obtained the frequency dependence of the imaginary part of the pseudo-dielectric function shown in Fig. 2 for two different pressures. This figure demonstrates that the reflectivity peak near 1.15

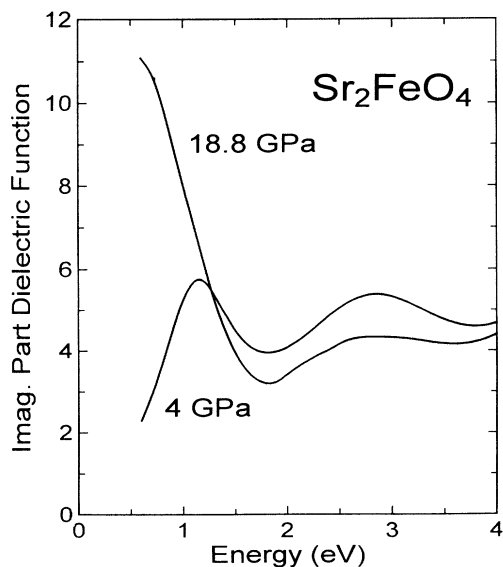


FIG. 2. Imaginary part of the pseudodielectric function of  $\text{Sr}_2\text{FeO}_4$  at two different pressures (see text for details).

eV at 4 GPa corresponds to an optical transition centered at about the same energy. Furthermore, the increase in near-infrared reflectivity at high pressure corresponds to a significant increase in oscillator strength at energies below 1 eV.

Raman spectra of  $\text{Sr}_2\text{FeO}_4$  at different temperatures are shown in Fig. 3. At room temperature we observe three Raman lines at 206, 281, and  $509\text{ cm}^{-1}$ . By comparing to Raman spectra of related compounds,<sup>26</sup> these modes can be attributed to a strontium vibration of  $A_{1g}$  symmetry, an oxygen  $E_g$  mode, and an oxygen  $A_{1g}$  mode, respectively. In addition, the Raman spectra show a broad band at room temperature which is centered near  $350\text{ cm}^{-1}$ . Upon cooling this band narrows considerably. From Raman measurements in parallel and crossed polarization we conclude that it has mainly  $A_1$  symmetry. In the room temperature Raman spectra of the  $^{18}\text{O}$ -substituted sample of  $\text{Sr}_2\text{FeO}_4$  the phonon modes at 206, 281, and  $509\text{ cm}^{-1}$  are shifted by  $-0.5\%$ ,  $-4.4\%$ , and  $-4.6\%$  to lower frequencies, which confirms the above assignment of the phonons. The additional broad band behaves like the oxygen-derived phonons and shifts by  $-4.4\%$ .

We have fitted a Gaussian line shape to the  $350\text{ cm}^{-1}$  Raman band in order to determine the temperature dependence of the position, linewidth, and integrated intensity. The results are shown in Fig. 4. The integrated intensity [normalized to the sum of intensities of the phonon Raman lines, see inset in Fig. 4(b)] is almost independent of temperature. The main temperature effect is a narrowing of the  $350\text{ cm}^{-1}$  band upon cooling, going along with an apparent blueshift which is larger than the temperature dependence of the normal phonon frequencies.

Figure 5 shows low-temperature Raman spectra of  $\text{Sr}_2\text{FeO}_4$  measured at different pressures. The corresponding pressure dependence of the Raman line frequen-

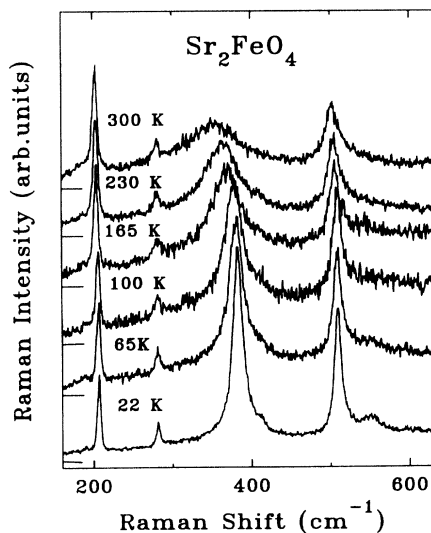


FIG. 3. Zero-pressure unpolarized Raman spectra of polycrystalline  $\text{Sr}_2\text{FeO}_4$  measured at different temperatures. The excitation wavelength is 514 nm.

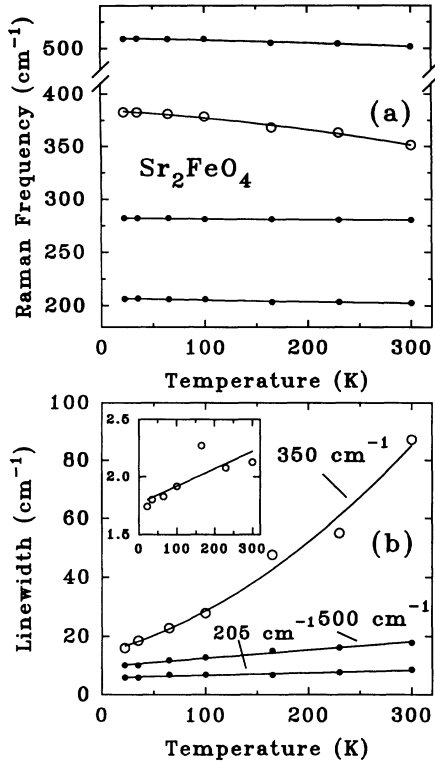


FIG. 4. Temperature dependence of (a) the frequency and (b) linewidth and integrated intensity (inset, arbitrary units) of the  $350\text{ cm}^{-1}$  and other Raman lines as obtained from fits with a Gaussian line profile.

cies is displayed in Fig. 6(a), and the pressure coefficients for the various modes are summarized in Table I. Under pressure, the three phonon Raman lines increase in frequency at a rate similar to that observed for the structurally related compound  $\text{Sr}_2\text{TiO}_4$ .<sup>26</sup> The  $350\text{ cm}^{-1}$  band, on the other hand, shows a *negative* frequency shift under pressure. Furthermore, this band starts to lose in-

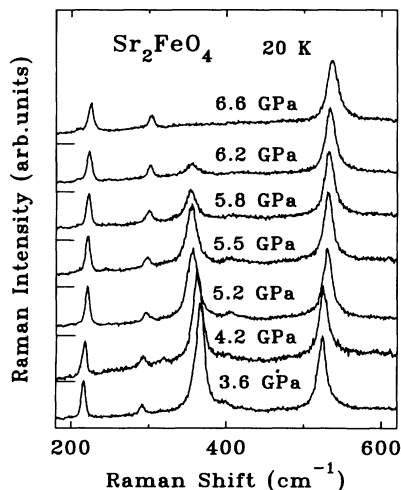


FIG. 5. Low-temperature Raman spectra of  $\text{Sr}_2\text{FeO}_4$  at different pressures.

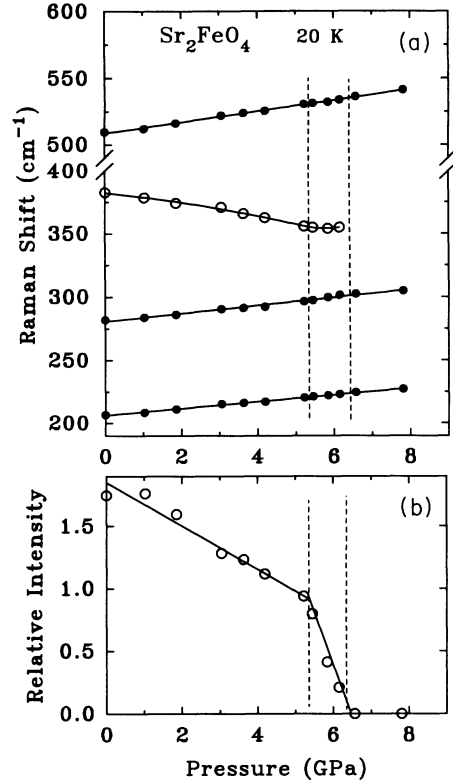


FIG. 6. (a) Pressure dependence of the Raman frequencies of  $\text{Sr}_2\text{FeO}_4$ . (b) Integrated intensity of the  $350\text{ cm}^{-1}$  mode in  $\text{Sr}_2\text{FeO}_4$  normalized to the sum of the phonon Raman line intensities.

tensity at about 5 GPa [see Fig. 6(b)] and is not observed any more above 6 GPa. Also, the corresponding broad band in the room temperature spectrum is not observed above 6 GPa.

#### IV. DISCUSSION

First of all it is noted that neither the optical spectra up to 38 GPa nor the Raman spectra up to 17 GPa show any evidence of a pressure-induced high-spin-low-spin transition of the  $\text{Fe}^{4+}$  ion. In this case more drastic changes in the whole optical excitation spectrum or at least in the oxygen phonon modes are expected.

The pressure-induced changes seen in optical reflectivity, in particular the increase of the low-energy oscillator strength, point to the possibility of an insulator-metal transition near 6 GPa followed by a continuous increase

TABLE I. Raman frequencies and linear pressure coefficients for  $\text{Sr}_2\text{FeO}_4$  measured at 20 K. Frequencies are given in  $\text{cm}^{-1}$ , and pressure coefficients in  $\text{cm}^{-1}/\text{GPa}$ .

$\nu_0$	$d\nu/dP$	$d(\nu/\nu_0)/dP$
206.3(3)	2.70(6)	0.0131
280.8(6)	3.14(13)	0.0112
383.2(9)	-4.7(3)	-0.0123
508.7(5)	4.17(8)	0.0082

of the free carrier density at higher pressures with saturation at about 20 GPa. We note that the reflectivity spectrum near 19 GPa is similar to that measured for  $\text{YBa}_2\text{Cu}_3\text{O}_{6.8}$  under similar experimental conditions.<sup>27</sup> The low-energy limit of the present reflectivity measurements is at 0.5 eV, and the absolute magnitude of the maximum reflectivity at this energy is still rather low. Therefore we cannot rule out the possibility of a low-energy gap persisting in the electronic excitation spectrum. Nevertheless, the increase in oscillator strength in the near-infrared spectral range shows that the system is pushed towards degeneracy with a less localized ground state.

The interpretation of the near-infrared transition seen near 1.15 eV at 4 GPa plays a key role in assigning the new ground state. From the general systematics of the electronic properties of TM compounds<sup>4</sup> and molecular orbital calculations on  $[\text{FeO}_6]^{8-}$  and  $[\text{Fe}_2\text{O}_{11}]^{14-}$  units<sup>28</sup> it is evident that chemical bonding in oxoferrates(IV) is characterized by strong covalent interactions between the Fe 3*d* and O 2*p* orbitals. Within the cluster CI approach the wave function of the high-spin state for a  $[\text{FeO}_6]^{8-}$  cluster is written as<sup>12</sup>

$$\Psi(^5E_g) = a|d^4, ^5E_g\rangle + b|d^5L^{-1}, ^5E_g\rangle. \quad (1)$$

For  $\text{SrFeO}_3$  the charge-transfer energy  $\Delta = E(d^5L^{-1}) - E(d^4)$  was shown to be about zero if defined with respect to the center of gravity of states belonging to each configuration or, as a consequence of the large exchange stabilization of the  $d^5$  configuration, even negative if defined with respect to the lowest-energy multiplet levels. In view of the similar Fe-O bond distances it is likely that the cluster model parameters are not very different for  $\text{Sr}_2\text{FeO}_4$ . From these data it is expected that the strontium ferrates(IV) are in or near the region of *p*-band metals of the Zaanen-Sawatzky-Allen (ZSA) phase diagram.<sup>8</sup>  $\text{SrFeO}_3$  is metallic whereas  $\text{Sr}_2\text{FeO}_4$  is a semiconductor at ambient pressure. We suggest that the insulating ground state of  $\text{Sr}_2\text{FeO}_4$  is due to the formation of a local  $^5E_g$  state (with respect to  $O_h$  symmetry) of mixed  $d^5L^{-1}$  and  $d^4$  character which is split off from a  $d^5L^{-1}$  continuum due to hybridization between the charge-transfer  $d^5L^{-1}$  and the ionic  $d^4$  states.

In a similar way the insulating behavior of the formal  $\text{Cu}^{3+}$  oxide  $\text{NaCuO}_2$  was explained by the formation of a local  $^1A_1$  state of primarily  $d^9L^{-1}$  character which is split off from the  $d^9L^{-1}$  continuum via hybridization with the excited  $3d^8$  configuration of ionic  $\text{Cu}^{3+}$ .<sup>7</sup> In the case of  $\text{NaCuO}_2$  the Cu-O-Cu bond angle is  $90^\circ$  which yields a weak intercluster coupling and thus favors the formation of the local singlet state. On the other hand, the three-dimensional perovskite  $\text{LaCuO}_3$  with Cu-O-Cu angles of  $180^\circ$  is metallic. The electronic structure of  $\text{Cu}^{3+}$  oxides has been analyzed quantitatively by impurity model calculations<sup>29</sup> which also have been used previously to describe the photoionization states of  $\text{Cu}^{2+}$  oxides.<sup>30</sup> The calculations demonstrate that the existence of the local singlet state depends on the relative magnitudes of the cluster parameters and the bandwidth  $W_p$ .

Within the above electronic structure model for  $\text{Fe}^{4+}$

compounds, the excitation near 1.15 eV seen in the optical spectrum of  $\text{Sr}_2\text{FeO}_4$  at low pressure can be assigned to the transition from the local  $^5E_g$  ground state to the  $d^5L^{-1}$  continuum. The main effect of pressure is an increase of the hybridization strength  $T_{pd}$  and the bandwidth  $W_p$ . If the increase in  $W_p$  is the dominant effect, a narrowing of the gap and eventually an insulator-metal transition occur. This would qualitatively explain the pressure-induced changes observed in the optical response.

Alternatively, the possibility of a pressure-induced charge density wave (CDW) needs to be considered. Mössbauer spectra of  $\text{CaFeO}_3$  at ambient pressure prove the existence of two electronically different sites which have been interpreted in terms of a  $2\text{Fe}^{4+} \rightarrow \text{Fe}^{3+} + \text{Fe}^{5+}$  or more likely a  $2\text{Fe}^{4+} \rightarrow \text{Fe}^{(4-\delta)+} + \text{Fe}^{(4+\delta)+}$  charge disproportionation.<sup>13</sup> As discussed by ZSA, strong fluctuations between  $d^n$ ,  $d^{n+1}L^{-1}$ ,  $d^nL^{-1}$ , and  $d^{n+1}$  states, i.e., between  $d^4$ ,  $d^5L^{-1}$ ,  $d^4L^{-1}$ , and  $d^5$  states in the case of interest, occur in an intermediate region of their phase diagram near the insulator-metal borderline.<sup>8</sup> In this region their model leads to unphysical negative energy gaps. It was suggested that a nonuniform charge distribution may be lowest in energy. The oxoferrates(IV) revealing a formal charge disproportionation may correspond to this intermediate region. The Mössbauer spectra of  $\text{Sr}_2\text{FeO}_4$  at ambient pressure exclude a nonuniform charge distribution. A pressure-induced transition to a CDW state, however, may be possible. The increase in near-infrared reflectivity would then be due to low-energy charge-transfer excitations in the CDW phase.

We now discuss the extra Raman mode near  $350 \text{ cm}^{-1}$ , which is the most intense feature in the Raman spectra. The band reveals the same isotope shift of  $-4.4\%$  as the oxygen-derived phonons. The cross-polarization experiment shows that it has  $A_1$  symmetry. Isotope shift and symmetry rule out an interpretation in terms of a ligand-field excitation between the  $^5B_{1g}$  ground state and the  $^5A_{1g}$  excited state which arise from the formal  $d^4$  configuration of tetravalent Fe centered in a slightly elongated octahedron. Also, an interpretation in terms of two-magnon scattering is not consistent with the experimental observations. We conclude that the band involves oxygen phonon modes with anions vibrating in the *z* direction. Such a vibration in addition to the oxygen  $A_{1g}$  mode at  $509 \text{ cm}^{-1}$  is not expected for the  $\text{K}_2\text{NiF}_4$ -type crystal structure.<sup>26</sup>

Additional phonon Raman scattering may arise from spin degrees of freedom. This effect has been observed in the Raman spectra of some magnetic semiconductors as, e.g., the europium chalcogenides.<sup>31,32</sup> Broad features in the Raman spectra of the paramagnetic phases were interpreted in terms of scattering from a weighted phonon density of states induced by spin disorder. In the magnetically ordered phases sharp bands are observed. These can be attributed to phonons which are forbidden in the chemical but become allowed in the magnetic unit cell. Drastic changes occur in the vicinity of the magnetic phase transition reflecting the change from spin disorder to a spin-ordered state. In the case of  $\text{Sr}_2\text{FeO}_4$  the main temperature effects are a sharpening and a blue-

shift of the band maximum upon cooling, but there are no pronounced changes around  $T_N \approx 60$  K. Thus, if the additional Raman band in  $\text{Sr}_2\text{FeO}_4$  arises from spin-induced phonon scattering, the continuous changes across  $T_N$  would indicate a gradual transition from spin disorder to the ordered phase. The spin fluctuations above  $T_N$  must, however, be rather rapid as there is no evidence for local spin order above  $T_N$  in the Mössbauer spectra.<sup>15</sup>

A second possibility for the interpretation of the  $350\text{ cm}^{-1}$  band would be in terms of a small structural distortion like the displacement of Fe ions from the center positions of the oxygen octahedra. The large linewidth at temperatures above 200 K indicates that such a displacement is either dynamically or statically disordered, which may prevent its observation in x-ray and neutron diffraction studies. The sharpening of the band on cooling corresponds either to a slowing down of the dynamics or to a gradual disorder-order transition. Possible vibrations involving the motion of oxygen anions in the  $z$  direction which could become Raman active by symmetry lowering are the  $B_{2u}$  and  $A_{2u}$  modes in  $D_{4h}$  symmetry. The former is a silent mode and involves the antiphase motion of the  $O_x$  and  $O_y$  plane oxygen atoms, whereas the latter is infrared active and involves the in-phase motion of  $O_x$  and  $O_y$  atoms. One might suspect that other vibrations should also become Raman active in this case. It is noted that the low-temperature Raman spectra reveal additional weak bands the origin of which is not yet clear. In this context it is remarkable that complicated Mössbauer spectra of the magnetically ordered phase of  $\text{Sr}_2\text{FeO}_4$  were observed which have been interpreted in terms of local structural distortions<sup>15</sup> or a complicated spin structure.<sup>16</sup> A low-temperature neutron diffraction study does not show any evidence for structural distortions.<sup>16</sup>

The additional Raman band disappears just in the same pressure range where the near-infrared oscillator strength starts to increase. This may be an indication for a correlation between changes in electronic structure and the loss of Raman activity. If the phonon scattering near  $350\text{ cm}^{-1}$  is spin induced, the pressure-driven disappearance of the band would indicate a transition from a localized to an itinerant electronic ground state with simultaneous loss of localized spins. On the other hand, if the band originates from a structural distortion the negative pressure shift and the disappearance around 5.5 GPa would correspond to a continuous reduction and a subsequent discontinuous disappearance of the Fe ion displacement from the center positions within the octahedra.

## V. SUMMARY AND CONCLUDING REMARKS

We have studied the pressure dependence of the optical reflectivity and Raman spectra of  $\text{Sr}_2\text{FeO}_4$ , a semiconducting compound with the two-dimensional  $\text{K}_2\text{NiF}_4$  structure and with iron in the high formal oxidation state of +4. External pressure leads to a redshift of the lowest optical transition near 1.2 eV and an increase in the near-

infrared reflectivity starting near 6 GPa. We propose that the insulating ground state of  $\text{Sr}_2\text{FeO}_4$  is due to the formation of a local ligand-field-like  ${}^5E_g$  state (referred to  $O_h$  symmetry) of mixed  $d^4$  and  $d^5L^{-1}$  character which is split off from a  $d^5L^{-1}$  continuum. Within this model external pressure increases the bandwidth and leads to an insulator - metal transition which would then account for the increase in near-infrared oscillator strength above 6 GPa. Alternatively, a pressure-induced valence disproportionation may occur near 6 GPa. The ambient pressure Raman spectra show, in addition to the vibrational modes which are expected for the  $\text{K}_2\text{NiF}_4$  structure, an intense oxygen phonon mode of  $A_1$  symmetry near  $350\text{ cm}^{-1}$ . This mode is broad at 300 K and develops into a sharp structure upon cooling to 20 K. Spin-induced phonon scattering or small structural distortions are considered as possible origins for the Raman activity of this mode. It is suggested that its pressure-driven disappearance near 5.5 GPa may be related to the electronic changes occurring in this pressure range.

Further experiments are required for a reliable assignment of the additional phonon mode in the low-pressure Raman spectra of  $\text{Sr}_2\text{FeO}_4$ . Also, it is quite obvious from the present results that a pressure-dependent Mössbauer effect study would be highly desirable to check the possibility of a valence disproportionation near 6 GPa and also to investigate the behavior of the magnetic ordering under pressure.

Strontium ferrates with tetravalent iron reveal an interesting variety of electronic properties. The three-dimensional perovskite  $\text{SrFeO}_3$  has a high electronic conductivity and may be an example for a correlated metal.  $\text{Sr}_2\text{FeO}_4$  with the two-dimensional  $\text{K}_2\text{NiF}_4$  structure is a semiconductor at ambient pressure which seems to be driven towards an insulator-metal transition under high pressure. Furthermore, in the Ruddlesden-Popper-type phase  $\text{Sr}_3\text{Fe}_2\text{O}_7$ , the crystal structure of which consists of two-dimensional sheets of  $\text{FeO}_6$  double octahedra, a nonuniform charge distribution state, formally expressed as  $2\text{Fe}^{4+} \rightarrow \text{Fe}^{3+} + \text{Fe}^{5+}$ , is found.<sup>13,16</sup> In this series of compounds the coordination geometries and Fe-O bond lengths are not very different. Accordingly, the intra-cluster electronic structure parameters for an  $[\text{FeO}_6]^{8-}$  unit are expected to be nearly the same. The electronic behavior of the strontium ferrates(IV) is presumably determined by the different bandwidths arising from the different methods of intercluster coupling in the respective crystal structures. This is a unique example for the "chemical control of physical parameters"<sup>5</sup> determining the electronic structure.

## ACKNOWLEDGMENTS

The authors thank U. Oelke for performing the reflectivity measurements. We have enjoyed stimulating discussions with M. Cardona and T. Ruf. A.G. gratefully acknowledges financial support from the Alexander von Humboldt foundation and Max Planck Society. Part of this work is supported by EC Grant No. SC1\*-CT91-0751 (TSTS).

- \*On leave from Institute of Crystallography, Russian Academy of Science, Moscow, Russia.
- <sup>1</sup>N. F. Mott, *Metal-Insulator Transitions* (Taylor and Francis, London, 1974).
- <sup>2</sup>B. H. Brandow, *Adv. Phys.* **26**, 651 (1977).
- <sup>3</sup>J. Zaanen and G. A. Sawatzky, *J. Solid State Chem.* **88**, 8 (1990).
- <sup>4</sup>A. E. Bocquet, T. Mizokawa, T. Saitoh, H. Namatame, and A. Fujimori, *Phys. Rev. B* **46**, 3771 (1992); A. E. Bocquet, T. Saitoh, T. Mizokawa, and A. Fujimori, *Solid State Commun.* **83**, 11 (1992).
- <sup>5</sup>A. Fujimori, *J. Phys. Chem. Solids* **53**, 1595 (1992).
- <sup>6</sup>P. A. Cox, *Transition Metal Oxides* (Clarendon Press, Oxford, 1992).
- <sup>7</sup>T. Mizokawa, H. Namatame, A. Fujimori, K. Akeyama, H. Kondoh, H. Kuroda, and N. Kosugi, *Phys. Rev. Lett.* **67**, 1638 (1991).
- <sup>8</sup>J. Zaanen, G. A. Sawatzky, and J. W. Allen, *Phys. Rev. Lett.* **55**, 418 (1985).
- <sup>9</sup>For a review, see M. Takano and Y. Takeda, *Bull. Inst. Chem. Res. Kyoto Univ.* **61**, 406 (1983).
- <sup>10</sup>J. B. MacChesney, R. C. Sherwood, and J. F. Potter, *J. Chem. Phys.* **43**, 1907 (1965).
- <sup>11</sup>P. K. Gallagher, J. B. MacChesney, and D. N. E. Buchanan, *J. Chem. Phys.* **41**, 2429 (1964).
- <sup>12</sup>A. E. Bocquet, A. Fujimori, T. Mizokawa, T. Saitoh, H. Namatame, S. Suga, N. Kimizuka, Y. Takeda, and M. Takano, *Phys. Rev. B* **45**, 1561 (1992).
- <sup>13</sup>M. Takano, N. Nakanishi, Y. Takeda, S. Naka, and T. Takada, *Mater. Res. Bull.* **12**, 923 (1977).
- <sup>14</sup>Y. Takeda, S. Naka, M. Takano, T. Shinjo, T. Takada, and M. Shimada, *Mater. Res. Bull.* **13**, 61 (1978).
- <sup>15</sup>P. Adler, *J. Solid State Chem.* **108**, 275 (1994).
- <sup>16</sup>S. E. Dann, M. T. Weller, D. B. Currie, M. F. Thomas, and A. D. Al-Rawwas, *J. Mater. Chem.* **3**, 1231 (1993).
- <sup>17</sup>S. E. Dann, M. T. Weller, and D. B. Currie, *J. Solid State Chem.* **92**, 237 (1991).
- <sup>18</sup>C. N. R. Rao, P. Ganguly, K. K. Singh, and R. A. Mohan Ram, *J. Solid State Chem.* **72**, 14 (1988).
- <sup>19</sup>M. Takano, S. Nasu, T. Abe, K. Yamamoto, S. Endo, Y. Takeda, and J. B. Goodenough, *Phys. Rev. Lett.* **67**, 3267 (1991).
- <sup>20</sup>H. Tups and K. Syassen, *J. Phys. C* **14**, 253 (1984).
- <sup>21</sup>M. Hanfland, M. Alouani, K. Syassen, and N. E. Christensen, *Phys. Rev. B* **38**, 12 864 (1988).
- <sup>22</sup>U. Venkateswaran, K. Syassen, Hj. Mattausch, and E. Schönherr, *Phys. Rev. B* **38**, 7105 (1988).
- <sup>23</sup>H. K. Mao, J. Xu, and P. M. Bell, *J. Geophys. Res.* **91**, 4673 (1986).
- <sup>24</sup>R. A. Noack and W. B. Holzapfel, in *High Pressure Science and Technology*, edited by K. D. Timmerhaus, and M. S. Barber (Plenum, New York, 1979), Vol. 1, p. 748; D. M. Adams, R. Appleby, and S. K. Sharma, *J. Phys. E* **9**, 1140 (1976); I. F. Silvera and R. J. Wijngarden, *Rev. Sci. Instrum.* **56**, 121 (1985).
- <sup>25</sup>For a discussion of sum rules, see, e.g., D. Y. Smith, in *Handbook of Optical Constants of Solids*, edited by E. D. Palik (Academic, New York, 1985).
- <sup>26</sup>U. Venkateswaran, K. Strössner, K. Syassen, G. Burns, and M. W. Shafer, *Solid State Commun.* **64**, 1273 (1987).
- <sup>27</sup>M. Garriga, U. Venkateswaran, K. Syassen, J. Humlicek, M. Cardona, Hj. Mattausch, and E. Schönherr, *Physica C* **153-155**, 643 (1988).
- <sup>28</sup>H. Adachi and M. Takano, *J. Solid State Chem.* **93**, 556 (1991).
- <sup>29</sup>T. Mizokawa, A. Fujimori, H. Namatame, K. Akeyama, and N. Kosugi, *Phys. Rev. B* **49**, 7193 (1994).
- <sup>30</sup>H. Eskes and G. A. Sawatzky, *Phys. Rev. Lett.* **61**, 1415 (1988).
- <sup>31</sup>G. Güntherodt and R. Zeyer, in *Light Scattering in Solids*, edited by M. Cardona and G. Güntherodt (Springer-Verlag, Berlin, 1984), Vol. IV, p. 203.
- <sup>32</sup>G. Güntherodt and R. Merlin, in *Light Scattering in Solids* (Ref. 31), p. 243.